Preprints, 10th IFAC International Symposium on
Advanced Control of Chemical Processes
Shenyang, Liaoning, China, July 25-27, 2018

Model predictive control of fuel cells system within hybrid renewable energy generation

Scarlett Chen[a,b], Min-Sen Chiu[a], Xiaonan Wang[a] *
[a]*Department of Chemical and Biomolecular Engineering, National University of Singapore, Singapore 117585*
[b]*University of Alberta, 116 St & 85 Ave, Edmonton, AB T6G 2R3, Canada*
* Corresponding author. +65 6601 6221 (Tel) +65 6779 1936 (Fax) chewxia@nus.edu.sg (Email)

Abstract
This paper presents model predictive control (MPC) strategies with a shrinking horizon approach to track local control systems when subject to supervisory trajectories. The supervisory trajectories are generated using economic receding horizon optimization based on energy management in energy-intensive industries (e.g., chlor-alkali process) with a hybrid renewable energy system (HRES), including solar, wind, and fuel cell sub-systems to provide sustainable power supply. A planer solid oxide fuel cell system is adopted in this study, and its power output is regulated using a constrained shrinking horizon MPC controller. The feasibility of MPC control algorithm in regulating energy sub-systems within a supervisory MPC framework will be studied and evaluated at different parameters. The main contribution of this paper is to provide practical control options when addressing technical viability concerns of hybrid energy system implementation.

1. Introduction

Distributed energy generation can create tremendous energy cost savings in replacement of traditional centralized productions. Robust and reliable control of hybrid renewable energy systems (HRES) are essential requirements to building a flexible infrastructure in future energy supplies and is a research direction studied by extensive literature [1] [2]. As one of the highest energy consuming processes, the chlor-alkali industry converts electrical energy into chemical energy whilst producing chlorine, caustic soda and hydrogen through the electrolysis of sodium chloride solution [3]. With the growth of hydrogen economy, benefits of using hydrogen as a supplementary energy carrier are realized and supported by increasingly more public policies and economic and environment conditions [4]. Amongst these, waste-to-energy plants generate considerable net environmental and economic profits. Municipal and ecological wastes such as wastewater and by-products form chlor-alkali processes are converted into production of energy, in the forms of electricity, heat, and/or energy carriers like hydrogen [5]. These production, termed "waste hydrogen" can be sold for revenue, or recycled within the plant to satisfy other powering requirements. A study conducted in 2011 has shown that over 150 manufacturing facilities in the U.S. have the potential of recovering hydrogen but are currently not practicing it. There are also 40,000 waste treatment facilities (e.g. wastewater treatment, anaerobic digester, landfill gases) that could be modified to produce hydrogen. Amongst these facilities, the equivalent hydrogen produced is approximately 17.8 trillion cubic feet, which can be translated to powering 210 million cars. In addition, 389,000 metric tons of hydrogen is produced from chlor-alkali plants in the U.S. annually, and 1,438,000 metric tons of chlor-alkali hydrogen produced worldwide – 15% of which is vented into the atmosphere without recovering. The vented hydrogen produces potential electricity of 420 MW from fuel cells at 50% efficiency year [6] [7]. Tremendous numbers have demonstrated the opportunities of hydrogen economy, and the same transferrable benefits apply to other nations worldwide where recovery of waste hydrogen is possible. Renewable hydrogen produced from waste sources is the most cost-effective and efficient process; it turns waste assets into marketable products and/or aids in increasing operational efficiency within a plant, especially for an energy-intensive process like chlor-alkali electrolyzers. Moreover, having hydrogen storage helps reducing the intermittent production from renewable energy sources. During standby states, there will be no fuel consumption; and during high demand states, hydrogen production and storage allows rapid load following capability. Fuel cells provide a promising solution to recovering un-used electrolytic hydrogen as they take hydrogen as a fuel to convert chemical energy into electrical energy [8]. Tying hydrogen recycling to waste treatment plants along with distributed energy generation resources is a pioneering system design to maximize system efficiency and minimize environmental impacts.

This paper investigates the control and optimization within the distributed energy micro-grid with a heavy focus on the fuel cell component of the HRES. While optimizing the dispatch strategies between energy resources on a supervisory level is paramount to efficient plant operation, effective local control of the sub-systems to track the power reference provided by the supervisor is equally important to realize these optimizing strategies. Many past studies on the control of fuel cells [9] to enhance power system stability have been conducted [10] [11]. Model predictive control (MPC) is a powerful algorithm used in the field of control engineering; its advantages over other control methods include the simple design framework to realize multivariable control problems, as well as its ability to handle constraints on manipulated and controlled variables [12] [13]. This study aims to support the feasibility of hybrid systems by demonstrating the technical viability of one of the local control options. A constrained MPC framework is used to regulate the power output of a solid oxide fuel cell stack at the desired setpoint.

Operational optimization of the overall HRES structure with the chlor-alkali process will be introduced in Section 2. Integration of solid oxide fuel system is presented in Section 3. The formulation of MPC algorithm adapted for this study is shown in Section 4. Preliminary results of system responses upon implementation of MPC controllers at different tuning parameters are shown in Section 5. Conclusions and future directions are discussed in Section 6.

2. Supervisory Optimization of HRES

A chlor-alkali electrolyzer is introduced as the center energy consuming element of the hybrid renewable energy system, which interconnects independently-operated sub-systems such as solar and wind energy conversion systems, stacks of fuel cells with air supply and hydrogen storage tanks, and a smart grid system to allow purchasing and/or selling of electricity. X. Wang et al.'s previous work optimizes the power dispatch strategies of these sub-components to minimize economic and environmental costs using a receding horizon approach formulated in the discrete-time domain [3]. Operating and environmental cost, and product and electricity revenues are factors accounted for in its objective function. The optimization problem with respective variable constraints at each time instant, j, is formulated as follows:

$$
\begin{aligned}
& min \sum_{t=j}^{j+N\Delta} \alpha\left(\sum_i P_{i,ref}^t C_i^t\right) + \beta\left(\sum_i P_{i,ref}^t Cen_i^t\right) - \\
& \lambda_1\left(P_{gridSell,ref}^t C_{gridSell}^t\right) - \lambda_2\left(Q_{prod}^t C_{prod}^t\right) \\
& w.r.t. P_{PV,ref}^j, P_{wind,ref}^j, P_{FC_{in},ref}^j, P_{FC_{external},ref}^j, \\
& P_{gridBuy,ref}^j, P_{gridSell,ref}^j \\
& s.t. \forall\, t \in [j\Delta, (j+N)\Delta] \quad , \quad P_{req'd}^t = f(Q_{prod}^t) \quad ; \\
& P_{req'd}^t \le \sum_i P_{i,ref}^t - P_{gridSell,ref}^t; \\
& P_{i,min}^t \le P_{i,ref}^t \le P_{i,max}^t; \\
& \left|P_{i,ref}^{t+\Delta} - P_{i,ref}^t\right| \le dP_{i,max}; \\
& i = \{PV, wind, FC_{in}, FC_{external}, gridBuy\} \qquad (1)
\end{aligned}
$$

where α, β, λ_1 and λ_2 are the economic and environmental cost weighing factors penalizing each term. PV represents solar photovoltaic modules. N is horizon of hours each optimization is performed iteratively, Δ is the time interval at which optimization is updated (1 hour). $P_{i,ref}^t$ is power reference for each source. Cen_i^t, C_i^t are environmental and unit operation costs, FC_{in} is recovered hydrogen from fuel cell, $FC_{external}$ is stored hydrogen from externally. $C_{gridSell}^t$ and C_{prod}^t are unit prices to sell electricity and product. $P_{req'd}^t$, $P_{gridSell,ref}^t$ are electricity demanded and extra electricity generation sold back to the grid. Electricity demand is a function, f, of the required chlorine production Q_{prod}^t through the chlor-alkali electrolyzer plant model. $P_{i,min}^t, P_{i,max}^t$ are minimum and maximum energy output from source i . $dP_{i,max}$ is maximum energy change in power references between two consecutive optimization periods. This optimization problem is solved iteratively every hour. Demand response forecasted into the next 24 hours is also incorporated in the optimization in light of changing unit electricity cost. The demand for hourly production of chlorine can be varied depending on fluctuating unit cost, and can be controlled to reduce the average daily costs while meeting the total daily production requirement.

Each hour, the reference operating point for each power component calculated. The 24-hour power reference trajectory of the fuel cell sub-system are used as desired control set-points for the constrained MPC control algorithm.

3. System Design and Integration: Solid Oxide Fuel Cell (SOFC) Stack

A fuel cell generally consists of two electrodes and an electrolyte. Various types of fuel cell applications are available for different purposes [14] [15]. A solid oxide fuel cell is selected for this simulation study. It is possible to combine high-temperature SOFCs with low-temperature PEMFCs to construct a self-reforming system. SOFC stack can generate electrical power as well as stream of reformate gas that can be used as feed fuel for PEMFC [16]. This configuration can be investigated in future studies, but is not included in this work. For this study, in each cell of the stacked SOFC series, electrons released from hydrogen at the anode surface travel through the outer circuit and combine with oxygen at the cathode surface to produce oxide ions. Electrolyte allows oxide ions to pass and combine with H+ at the anode to form water. The following dynamic model of the fuel cell stack is adopted [17]:

$$
\begin{aligned}
& \Delta E = \left[\Delta E_o + \frac{RT}{2F}\ln\frac{p_{H_2}p_{O_2}^{0.5}}{p_{H_2O}}\right]; \tau_i^* = \frac{V}{K_i RT^*}; K_r = \frac{N_O}{4F} \\
& \Delta E_o = 1.2586 - 0.000252\, T_s \; ; \\
& V_s = N_o \Delta E - r_o exp\left[\alpha\left(\frac{1}{T_s} - \frac{1}{T_o}\right)\right] I \; ; \\
& \dot{p}_{H_2} = \frac{T_S}{\tau_{H_2}^* T^* K_{H_2}}\left(q_{H_2}^{in} - K_{H_2}P_{H_2} - 2K_r I\right) \\
& \dot{p}_{O_2} = \frac{T_S}{\tau_{O_2}^* T^* K_{O_2}}\left(q_{O_2}^{in} - K_{O_2}P_{O_2} - K_r I\right)
\end{aligned}
$$

$$\dot{p}_{H_2O} = \frac{T_S}{\tau^*_{H_2O}T^*K_{H_2O}}(q^{in}_{H_2O} - K_{H_2O}P_{H_2O} + 2K_rI)$$
$$\dot{T_S} = \frac{1}{m_sC_{ps}}\Big[\sum q^{in}_i \int_{T_{ref}}^{T_{in}} C_{p,i}(T)dT - \sum q^{out}_i \int_{T_{ref}}^{T_s} C_{p,i}(T)dT - 2K_rI\Delta\widehat{H^o_r} - V_sI\Big]$$
$$P = V_s * I;\ I = \varepsilon * \frac{q^{in}_{H_2}}{2*K_r},\ \varepsilon = \frac{q^{consumed}_{H_2}}{q^{in}_{H_2}} \quad (2)$$

where i represents components H_2, O_2, H_2O; p_i, T_S, q^{in}_i , q^{out}_i, $C_{p,i}$, K_i are the partial pressure, stack temperature, inlet and outlet molar flow rate, specific heat of gas, and valve molar constant of component i. V is the anode compartment volume. τ^*_i , is time constant obtained based on model parameters T^*, can be represented by $\tau^*_i = \tau_i|_{T_S=T^*}$. m_s and C_{ps} are the mass specific heat and average specific heat of fuel cell materials excluding gases. $\Delta\widehat{H^o_r}$ is the specific heat of reaction. I, N_O, and V_s are the load current, number of cells in the stack, and overall stack voltage. P is the power generated from the stack. F is Faraday's constant. r_o and α are the internal resistance at T_o and the resistance slope. ΔE is potential difference between electrodes, ΔE_o is standard cell potential, and ε is the hydrogen conversion efficiency. Model parameters and constants can be found in Murshed et. al [14].

The manipulated input is the inlet hydrogen flowrate. Power is the output variable, as electric power is generated from SOFC stack and is regulated to meet the desired set-points set by the supervisory optimization. The four state variables are $\dot{p}_{H_2}, \dot{p}_{O_2}, \dot{p}_{H_2O}, \dot{T_S}$. Assumptions in this simulation include ideal gases, no inlet water flow, constant $C_{p,i}$ (average across temperature range), and same inlet temperature for all gases.

4. Formulation of Linear Constrained MPC using Step Response Model

4.1 Convolution Model and Controller Design

As seen in many real-world processes, it is difficult to identify or select an appropriate model structure due to their complex and unusual dynamic behaviours. A discrete step response convolution model can be used to avoid such problems. The model coefficients can be obtained directly from experimental step tests without assuming a model structure. The convolution model can be represented in the form below [18]:

$$\hat{y}_k = y_0 + \sum_{i=1}^{M_T} a_i \Delta v_{k-i} \quad (3)$$

where $\hat{y}_k$ is the predicted output, y_0 is the initial output value, a_i are the step response coefficients, and $\Delta v_{(k-i)}$is the change in input at time $k - i$ up to M_T – the total simulation time required to achieve 99% of steady state, also known as "model horizon" in the MPC framework. The step response coefficients of the SOFC model are obtained from the open-loop output response at a sample time Δt when subject to a unit step input change around steady states. Alternatively, the step response model can be also represented by the sum of products of impulse response coefficients $h_i = a_i - a_{i-1}$ and input v_{k-i}at time instant $k - i$: $\hat{y}_k = y_0 + \sum_{i=1}^{M_T} h_i v_{k-i}$. Hence, in multi-step predictions, $\hat{y}_{k+j} = \hat{y}_{k+j-1} + \sum_{i=1}^{M_T} h_i \Delta v_{k-i}$.

The prediction error between actual plant output and predicted plant output using step response model is assumed to stay constant throughout the entire model horizon: $d_k = y_{k,plant} - \hat{y}_k = y^*_{k+1} - \hat{y}_{k+1} = y^*_{k+j} - \hat{y}_{k+j}$. This prediction error is accounted in the corrected output, $y^*_{k+j} = \hat{y}_{k+j} + d_k = \hat{y}_{k+j} + (y^*_{k+j-1} - \hat{y}_{k+j-1}) = y^*_{k+j-1} + \sum_{i=1}^{M_T} h_i \Delta v_{k-i}$. The corrected outputs along the prediction horizon can be represented in matrix formulations:

$$\begin{bmatrix} y^*_{k+1} \\ y^*_{k+2} \\ \vdots \\ y^*_{k+p} \end{bmatrix} = \begin{bmatrix} a_1 & 0 & 0 & \cdots & 0 \\ a_2 & a_1 & 0 & \cdots & 0 \\ \vdots & \vdots & \vdots & \ddots & \vdots \\ a_p & a_{p-1} & a_{p-2} & \cdots & a_{p-m+1} \end{bmatrix}_{p\times m} \times \begin{bmatrix} \Delta v_k \\ \Delta v_{k+1} \\ \vdots \\ \Delta v_{k+m-1} \end{bmatrix}_{m\times 1} + \begin{bmatrix} y_{k,plant} + s_1 \\ y_{k,plant} + s_1 + s_2 \\ \vdots \\ y_{k,plant} + s_1 + s_2 + \cdots + s_p \end{bmatrix}_{p\times 1}$$
$$S_j = \sum_{i=j+1}^{M_T} h_i\, \Delta v_{(k+j-i)}, for\ j = 1,2, \cdots p \quad (4)$$

where p the prediction horizon, m the control horizon are defined respectively as number of future corrected output predictions, and the number of future control actions used in each optimization control step. Thus, the output response predicted at $m \le p$ in vector form is: $[y^*_{k+1} \quad y^*_{k+2} \quad \cdots \quad y^*_{k+p}]^T = A\Delta V + B$, where A is the dynamic matrix including the step coefficients of the model, matrix B represents the contributions of all past control actions and output measurement feedback, ΔV is a vector containing changes in m future control actions computed at time instant k.

4.2 Constrained Optimization Problem

The convolution model provides the basis for MPC controller design based on the use of quadratic programming (QP) optimization. The objective function in the MPC optimization aims to minimize the residual between reference setpoint and corrected output. To formulate the objective function into a generalized equation utilized by QP, the MPC objective function is modified to be the following:

$$min_{\Delta V}\, J = [\Delta V(k)]^T H [\Delta V(k)] - h(k+1)^T \Delta V(k);$$
$$H = A^T W_1 A + W_2;\ \ h(k+1) = 2A^T W_1 (R - B)$$
$$R = [r_{k+1} \quad r_{k+2} \quad \cdots \quad r_{k+p}];$$
$$r_{k+i} \equiv Desired\ setpoint\ \ in\ the\ prediction\ horizon$$
$$W_1, W_2 \equiv \text{ weighting matrices of residuals \& incremental control actions respectively} \quad (5)$$

As it commonly occurs in practical control problems, inequality constraints on both controlled and manipulated variables arise due to physical limitations of the process. These constraints can be factored into the quadratic programming operation and represented in the general form:

$$\psi * x \le b;\ I \equiv Identity\ Matrix\ of\ m \times m;\ x = \Delta V;$$

$$\psi = \begin{bmatrix} -\Omega \\ -\Omega \\ -I \\ I \\ -A \\ A \end{bmatrix};\ \Omega = \begin{bmatrix} 1 & 0 & 0 & \cdots & 0 \\ 1 & 1 & 0 & \cdots & 0 \\ 1 & 1 & 1 & \cdots & 0 \\ \vdots & \vdots & \vdots & \ddots & 0 \\ 1 & \cdots & \cdots & \cdots & 1 \end{bmatrix}_{m\times m};\ b = \begin{bmatrix} -\beta_1 \\ \beta_2 \\ \beta_3 \\ \beta_3 \\ B - \beta_4 \\ \beta_5 - B \end{bmatrix}$$

$$\beta_1 = \begin{bmatrix} v_{min} - v_{k-1} \\ \cdots \\ v_{min} - v_{k-1} \end{bmatrix}_{m\times 1},\ \beta_2 = \begin{bmatrix} v_{max} - v_{k-1} \\ \cdots \\ v_{max} - v_{k-1} \end{bmatrix}_{m\times 1},$$

$$\beta_3 = \begin{bmatrix} \Delta v_{max} \\ \cdots \\ \Delta v_{max} \end{bmatrix}_{m\times 1}\ \beta_4 = \begin{bmatrix} y_{min} \\ \cdots \\ y_{min} \end{bmatrix}_{p\times 1}\ \beta_5 = \begin{bmatrix} y_{max} \\ \cdots \\ y_{max} \end{bmatrix}_{p\times 1} \quad (6)$$

The optimized control action, ΔV, is obtained by solving this QP problem by Matlab. Only the first control action Δv_k computed at time instant k is applied to the process, predicted output at the next time instant, $\hat{y}_{k+1}$, can be computed using Equation (3), and this optimization control repeats itself at each sample instant.

4.3 Shrinking Horizon Approach

For continuous processes with relatively rapid changes to track, conventional MPC controller using a receding horizon framework (similar to the algorithm deployed in the supervisory optimization) is robust and appropriate. In this study, the frequency of setpoint update is dictated by how often the optimization supervisor updates. Therefore, the available window for control is fixed to be 3,600 seconds. The controller aims for the same endpoint every period, similar to a batch process. Hence the prediction horizon, p, decreases incrementally as the time index approaches the end of the hour.. As the setpoint is updated hourly, p is reset to its original maximum value at the beginning of each hour, and the shrinking repeats over the next hourly horizon. The control objective is to reach the setpoint within the fixed window of one hour before the supervisory optimization refreshes.

5. Implementation and Analysis of MPC on SOFC Stack

5.1 Power Curves with Local Control

The reference curve of optimal power generation over 24 hours for the fuel cell stack is produced from HRES economic optimization. Constrained Model Predictive Control algorithm is applied to the system in two cases. over the 1st hour first, as well as over the 24-hour span. The constraints applied on the manipulated and controlled variables are as:

$$v_{min} = 0\frac{mol}{s}, v_{max} = 0.5\frac{mol}{s},$$
$$\Delta v_{max} = 0.5\frac{mol}{s}, y_{min} = 0W,$$
$$y_{max} = 2.193 \times 10^4 W$$

With fixed sampling time, the end point at each periodic hour that MPC controller aims for is also fixed. The MPC controller is tuned with respective to p, m, W_1, W_2, and constraints on manipulated and controlled variables. In all MPC controllers simulated in this study, m is selected to be 2. Larger p results in more conservative control and stabilized output, but increases computational effort. Shrinking horizon MPC algorithm helps to reduce computation. The starting value of p at time $k = 0$ is identical to the number of samples in the simulated hour, thus inversely proportional to the sampling time: $p(k = 0) = 1\ hour/\Delta t$. Hence, MPC controller can be tuned with respect to sampling time, Δt.

5.2 Steady Sate Estimations

Since the SOFC model is nonlinear, an adequate initial guess and a precise variable range for fast and accurate convergence are needed. Hence, constraints are imposed when solving for system steady states. Stack temperature range can be fixed based on the SOFC used; its upper bound is fixed at 1400K here. Additionally, logical constraints such as positive partial pressures are added.

5.3 Simulation Cases

Two realistic case studies corresponding to different time frames will be studied. To obtain the simulated plant feedback, open-loop response of the fuel cell system is recorded by solving the system of nonlinear ODEs at a time span identical to Δt of the MPC controller of each case. Initial power output is assumed to be 6.339 kW – the reference power value of the 24th hour from previous day, assuming the reference follows a daily cyclic pattern. Initial states and input are calculated in accordance to the initial power output. A step input double the initial steady state input value provided in each case below is introduced over the model horizon M_T. The output response is obtained as the deviation between observed output and initial output. This deviation is divided by the input change to obtain unit step open-loop response of the process. These unit step output at each time instant represents the step response model coefficients a_i used in MPC construction.

1) Fixed load power tracking for first hour

For the first study, controller design is for power set-point tracking of only the 1st hour of the day. Additionally, oxygen flow rate was assumed to be four times in excess i.e. oxygen flow rated is always double the hydrogen flow rate. A constant current load of 20 A is assumed. The initial states are calculated as follows:

$$I = 20A; v_{init} = q_{H_2}^{in}(0) = 0.1497\frac{mol}{s};$$
$$q_{O_2}^{in}(k) = 2 * q_{H_2}^{in}(k); y_{init} = P(0) = 6.91\ kW$$

The MPC control performance at two different sampling times, 10s and 60s, are evaluated for Case 1. Their performances are shown in Fig. 1. Only the first 30 minutes of the 1st hour is shown in Fig.1 to enlarge the response behaviours. Both MPC controllers are able to bring the system to its desired setpoint while meeting all constraints on manipulated and controlled variables, showing full competency in realizing local control of fuel cell system within the specified time frame. The overshoots by both controllers are marginal (with the highest peak under 0.24% deviation from the setpoint). In this case and in other cases where the interval of supervisory optimization may shrink to give more frequently updated setpoint references, rapid tracking with no overshoots helps reduce the operating costs of the fuel cell system further more.

2) Fixed efficiency power tracking for 24 hours

The second study is studied for complete 24 hours. The initial states were computed similar to that of the first study, but for this case, hydrogen conversion efficiency was assumed to be constant (ε= 0.4). The oxygen flow rate is assumed to be always double the hydrogen flow rate and hence in essence there is only one manipulated variable.

$$I = 0.4 * \frac{N_0}{4F};\ v_{init} = q_{H_2}^{in}(0) = 0.1119\frac{mol}{s};$$
$$q_{O_2}^{in}(k) = 2 * q_{H_2}^{in}(k);\ y_{init} = P(0) = 6.91\ kW$$

The results of the 24-hour MPC control are shown in Fig. 2 with the output response to a negative set-point change between hour 1 and 2 magnified. The MPC controller tracks the 24-hour setpoint trajectory rapidly without any unstable behaviour. One significant advantage of MPC is its capability for constrained control, therefore eliminating dramatic control actions from contributing to out-of-range output tracking. In a hybrid energy system with intensive and responsive demand and systematically optimized output, tracking within a constrained window is ideal. Since MPC also allows multivariable control, other variables in the SOFC system, such as oxygen flowrate and inlet temperature, can also be manipulated independently.

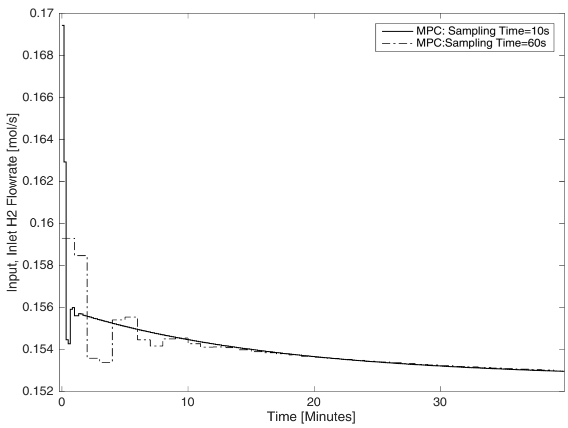

(a) Control Actions

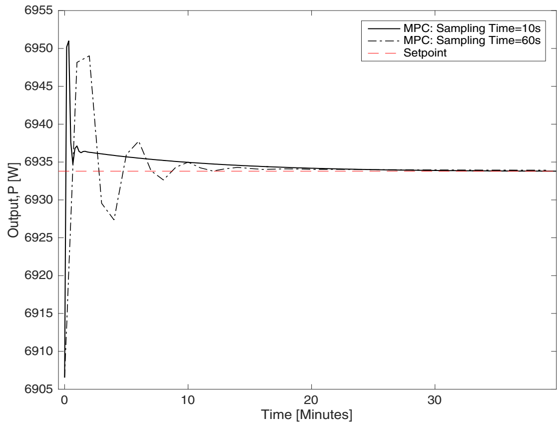

(b) Output Response

Fig. 1. Case 1 Simulation over 1st hour

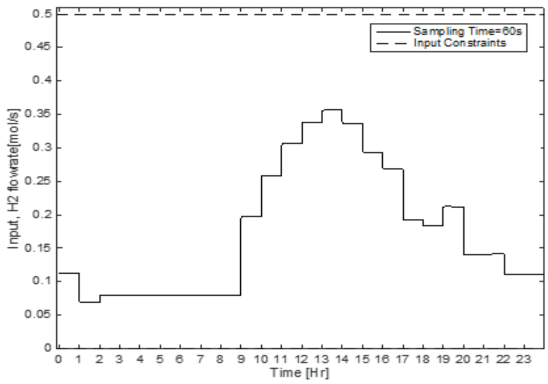

(a) Control Actions

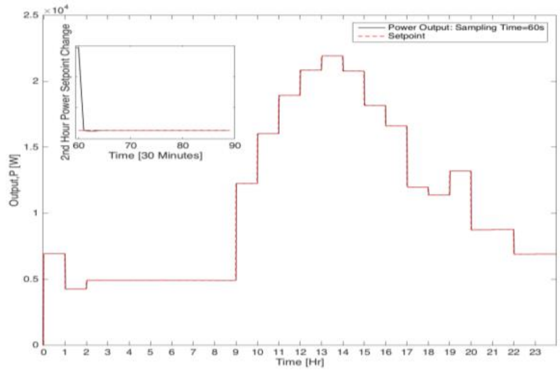

(b) Output Response

Fig. 2. Case 2 simulation over 24 hours at Δt=60s.

6. Conclusion and Future Work

This work investigated the effectiveness of shrinking horizon MPC controllers to realize the local control and tracking of power output of a SOFC stack. The supervisory power reference provided to the local controller is generated using receding horizon optimization, combining forecasting and demand management strategies over a 24-hour span. Both supervisor and local controller adopt a MPC framework in their objective functions. A nonlinear SOFC model is adopted, where its unit step response is simulated to construct a step response convolution model used for MPC framework design. Coupled with a shrinking horizon approach to ensure stability and reduce computational efforts, the model predictive controller with a sufficiently small sampling time yields robust variant-setpoints tracking performance, supporting the practical operability of the optimized energy system.

For future studies, the integration of different types of fuel cells (e.g., SOFC+PEMFC) as a self-reforming system can be investigated. Furthermore, the process model investigated in this case involves multiple variables and is nonlinear in nature. One future research direction is to design nonlinear MIMO MPC controllers using the nonlinear model directly, and conduct simulation studies to assess its performance.

References

[1] L. Che, "Mirogrids and Distributed Generation Systems: Control, Operation, Coordination and Planning," ProQuest LLC, Ann Arbor, 2015.

[2] Y.A. Mohamed, H.H. Zeinneldin, M.M.A Salama, "Seamless Formation and Robust Control of Distributed Generation Micogrids via Direct Voltage Control and Optimized Dynamic Power Sharing," *IEEE Transactions on Power Electronics,* vol. 27, no. 3, 2012.

[3] X. Wang, H. Teichgraeber, A. Palazoglu, N. H. El-Farra, "An Economic Receding Horizon Optimization Approach for Energy Management in the Chlor-Alkali Process with Hybrid Renewable Energy Generation," *Journal of Process Control,* vol. 24, pp. 1318-1327, 2014.

[4] I. Dincer and C. Acar, "Review and evaluation of hydrogen production methods for better sustainability," *ScienceDirect,* vol. 40, pp. 11094-11111, 2015.

[5] D.-Y. Lee, A. Elgowainy and Q. Dai, "Life cycle greenhouse gas emissions of hydrogen fuel production from chloralkali," *Applied Energy,* vol. 217, pp. 467-479, 2018.

[6] S. Satyapal, "Hydrogen and Fuel Cells Overview," in *DLA Worldwide Energy Conference*, National Harbor, MD , 2017.

[7] R. Cox, "Waste/By-Product Hydrogen," Fuel Cell and Hydrogen Energy Association, Washington, DC, 2011.

[8] G. Faita, A. Ottaviani, "Integration of Fuel Cells into Plants," *Fuel Cells Bulletin,* vol. 18, p. 16, 1999.

[9] C. P. M. Sorrentino, "Model-based development of low-level control strategies for transient operation of solid oxide fuel cell systems," *IET Renewable Power Generation,* vol. 6, no. 3, May 2012.

[10] K. Ro, S. Rahman, "Control of grid-connected fuel cell plants for enhancement of power system stability," *Renewable Energy,* vol. 28, no. 3, 2003.

[11] Y. Sun, S. Ghantasala, N. H. El-Farra, "Monitoring and Fault-Tolerant Control of Distributed Power Generation: Applicaiton of Solid Oxide Fuel Cells," in *American Control Conference*, Baltimore, 2010.

[12] L. Wang, Model Predictive Control System Design and Implementation Using Matlab, Melbourne: Springer-Verlag London Limited, 2009.

[13] D. M. Prett, C. E. Garcia, Fundamental Process Control, Butterworth-Heinemann, 1990.

[14] O'Hayre, Ryan P., Cha, Suk-Won, 1971-Colella, Whitney G., Prinz, F.B., Fuel Cell Fundamentals, Hoboken, New Jersey: John Wiley & Sons Inc, 2016.

[15] N. Sammes, "Ch.1 Solid Oxide Fuel Cells," in *Fuel Cell Technology: Reaching Towards Commercialization*, Golden, Colorado, Springer, 2006.

[16] W. Lin, "Waste Heat Recovery System for Fuel Cell System," TRRF05 Fuel Cell Technology, Lund University , Lund, Sweden, 2009.

[17] AKM M. Murshed, B. Huang, K. Nandakumar, "Control Relevant Modeling of Planer Solid Oxide Fuel Cell System," *Journal of Power Sources,* vol. 163, pp. 830-845, 2006.

[18] D. E. Seborg, T. F. Edgar, D. A. Mellichamp, Process Dynamics and Control, John Wiley & Sons, 1989.